SCIENTIFIC REPORTS

OPEN

SUBJECT AREAS:
NANOPARTICLES
ORGANIC-INORGANIC NANOSTRUCTURES
BATTERIES
SYNTHESIS AND PROCESSING

Received
5 March 2013

Accepted
14 May 2013

Published
29 May 2013

Correspondence and requests for materials should be addressed to L.W.C. (lwchen2008@sinano.ac.cn)

* These authors contributed equally to this work.

Ultrafine Sulfur Nanoparticles in Conducting Polymer Shell as Cathode Materials for High Performance Lithium/Sulfur Batteries

Hongwei Chen[1,2]*, Weiling Dong[1,3]*, Jun Ge[1], Changhong Wang[1,4], Xiaodong Wu[1], Wei Lu[1] & Liwei Chen[1]

[1]i-LAB, Suzhou Institute of Nano-Tech and Nano-Bionics (SINANO), Chinese Academy of Sciences, Suzhou 215123, China, [2]Institute of Chemistry, Chinese Academy of Sciences, Beijing 100190, China, [3]Institute of Semiconductors, Chinese Academy of Sciences, Beijing 100083, China, [4]Nano Science and Technology Institute, University of Science and Technology of China, Suzhou 215123, China.

We report the synthesis of ultrafine S nanoparticles with diameter 10 ~ 20 nm via a membrane-assisted precipitation technique. The S nanoparticles were then coated with conducting poly (3,4-ethylenedioxythiophene) (PEDOT) to form S/PEDOT core/shell nanoparticles. The ultrasmall size of S nanoparticles facilitates the electrical conduction and improves sulfur utilization. The encapsulation of conducting PEDOT shell restricts the polysulfides diffusion, alleviates self-discharging and the shuttle effect, and thus enhances the cycling stability. The resulting S/PEDOT core/shell nanoparticles show initial discharge capacity of 1117 mAh g^{-1} and a stable capacity of 930 mAh g^{-1} after 50 cycles.

Rechargeable lithium/sulfur (Li/S) batteries are potentially the next generation solution for high-density energy storage demands because sulfur cathodes have a high theoretical specific capacity of 1672 mAh g^{-1} and Li/S batteries have a theoretical energy density of 2600 Wh kg^{-1}, assuming complete conversion of sulfur to Li_2S[1]. Although recent works have made significant progresses[2–5], two major challenges still remain for this field: one is the low specific capacity due to high electrical resistivity of elementary S and the solid reduction products (Li_2S and Li_2S_2); the other is fast capacity fading owing to a shuttle effect, i.e. polysulfide intermediates formed during discharge/charge cycles dissolves in the electrolyte, diffuse to the anode, reacts with Li, and forms insoluble Li_2S and Li_2S_2 at the anodic region, which leads to the loss of active cathodic materials[6–8].

Earlier efforts of addressing these challenges have focused on loading sulfur into various porous carbon materials using ball milling and high temperature infiltration methods[9–12]. In these composites, porous carbon materials serve as conducting networks with large contact area to facilitate electron transport across sulfur. Furthermore, the porous structure helps to alleviate the shuttle effects by retaining polysulfide ions in the pores instead of dissolving into electrolyte[1,13]. However, these composites still exhibit degenerative electrochemical performance because of the diffusion and aggregation of sulfur. Recent developments with sulfur infiltrated into mesoporous and structured carbon materials with smaller pores using novel methods including liquid phase processing have resulted in better performance[14–17]. Meanwhile, surface encapsulation of the C-S composites has also been demonstrated to be an efficient method to promote the performance of Li/S batteries by suppressing the polysulfide shuttling effect[18,19].

While the porous carbon support is critically important in the C-S composite cathode material for Li/S batteries, it is electrochemically inactive and thus lowers the specific capacity of the cathode and the overall energy density of the battery. An alternative approach is to prepare sulfur nanoparticles to overcome the electrical insulating nature of sulfur without the need for support materials. Sulfur particles with nanometer-scaled diameter and high specific surface area require short electron transfer distance and also provide abundant electron transport active sites, which enables quick transfer of electrons to more sulfur. Similar approaches have succeeded in the commercialization of low-conductivity cathode materials for lithium ion batteries by reducing the particle size to hundreds of nanometers and coating with conducting carbon[20,21]. For Li/S batteries, submicrometer sulfur particles with graphene oxide wrapping and ~10 μm sulfur/polymer composite particles have

been prepared and shown promising high and stable specific capacities[16,22]. Considering the highly insulating nature of sulfur, it is thus intriguing to explore the nanoparticle approach and investigate the size effect truly down to nanometer scales.

In this work, we prepare ultrafine S nanoparticles with diameter in the 10 to 20 nm range using a unique membrane-assisted precipitation technique[23]. The S nanoparticles are then coated with poly (3,4-ethylenedioxythiophene) (PEDOT) to form S/PEDOT core/shell nanoparticles. The ultrasmall size of the S nanoparticles facilitates electron transport and the coating of PEDOT shells prohibits the dissolution of polysulfide ions to electrolyte. Thus a high initial discharge capacity up to 1117 mAh g^{-1} and a stable capacity of ~930 mAh g^{-1} over more than 50 cycles are achieved.

Results

Structural characterization. As illustrated in Fig. 1, high concentration of S in CS_2 solution is added to a large volume of ethanol through a microfiltration membrane with an average pore size of 100 nm. The S/CS_2 solution forms micro-droplets when passing the membrane. Since S is insoluble in ethanol, the S solute in micro-droplets precipitates into nanoparticles as soon as the droplets passes the membrane and mixes with the ethanol precipitant. Poly-vinylpyrimidine (PVP) in enthanol then functions as wrapping ligands to prevent the freshly formed S nanoparticles from aggregation. The advantage of this apprach is that the formation of S nanoparticles is restricted within each individual micro-droplets. In principle, the size of primary S nanoparticles is determined by the membrane pore size and the fluid dynamics across the membrane. After rinsing off excessive PVP, the S nanoparticles are re-dispersed in water and $FeCl_3$ was added. Fe^{3+} ions will adsorb onto the surfaces of S nanoparticles and then act as the oxidant to polymerize 3,4-ethylene dioxythiophene (EDOT) monomers to form S/PEDOT core/shell nanoparticles.

The TEM images of freshly obtained S nanoparticles are shown in Figure 2a and 2b. The particles show spherical shape with diameters ranging from 10 to 20 nm. The size distribution is confirmed by dynamic light scattering (DLS) analysis (Figure S1). The S nanoparticles disperse well in aqueous solution due to the PVP ligand, however, the PVP layer is not identifiable on the surface of S nanoparticles even in high resolution TEM micrograph (Figure 2b), which suggests that most of the PVP has been rinsed away and the nanoparticles composed S element mostly. The energy-dispersive X-ray (EDX) analysis verified the presence of sulfur element only (Figure S2).

After polymerization of EDOT monomer on the surface of S nanoparticle, an amorphous shell about 5 nm thick is formed around the S nanoparticles (Figure 2c and 2d). The EDX line profile along the dashed arrow in Figure 2d (Figure 2f) exhibits high S content in the core and low S content in the shell, confirming the core/shell structure of the particle. The FTIR spectrum of the S/PEDOT core/shell particle in Figure 2e shows characteristic peaks originating from both PEDOT and S. The peaks at 1527 and 1355 cm^{-1} are assigned to the C=C or C–C stretching of the quinoid structure and the ring stretching of the thiophene in PEDOT, respectively. The C–O–C antisymmetric stretching at 1209, 1148, and 1092 cm^{-1} and the C-S vibration at 987, 838, and 688 cm^{-1} arise from the ethylenedioxy group and the thiophene ring[24,25]. The peak at 1390 cm^{-1} stems from the characteristic absorption of sulfur. Three samples with different S contents were prepared as shown in Table S1 and Figure S3. For the core/shell nanoparticle whose electrochemical performance is studied in the following sections, the S content is 72 wt.%.

Nano-size effects. The sulfur nanoparticles and the S/PEDOT core/shell nanoparticles prepared above (dubbed as Nano-S and Nano-S@PEDOT, respectively, hereafter) are used as cathode materials in Li/S coin cells and their electrochemical performances are examined in Figure 3. Commercial powder sulfur (dubbed as CP-S hereafter) is used as a control material for comparison. SEM image of the CP-S sample shows a wide spread of particle size in the range of 1–50 μm (Figure S3a). The initial galvanostatic discharge/charge (GDC) profiles in Figure 3a show that Nano-S and Nano-S@PEDOT exhibit initial capacity of 1028 and 1117 mAh g^{-1}, respectively, while that of CP-S is 708 mAh g^{-1}.

Interestingly, the shape of the GDC profiles of CP-S and Nano-S are almost identical (Figure S4) and the ratio of first charge to first discharge capacity is the same, 105% for both CP-S and Nano-S cells. These consistencies suggest that the transformation from solid elementary S to soluble polysulfide intermediates and insoluble final forms of Li_2S_2 and Li_2S as well as the self-discharging of polysulfide

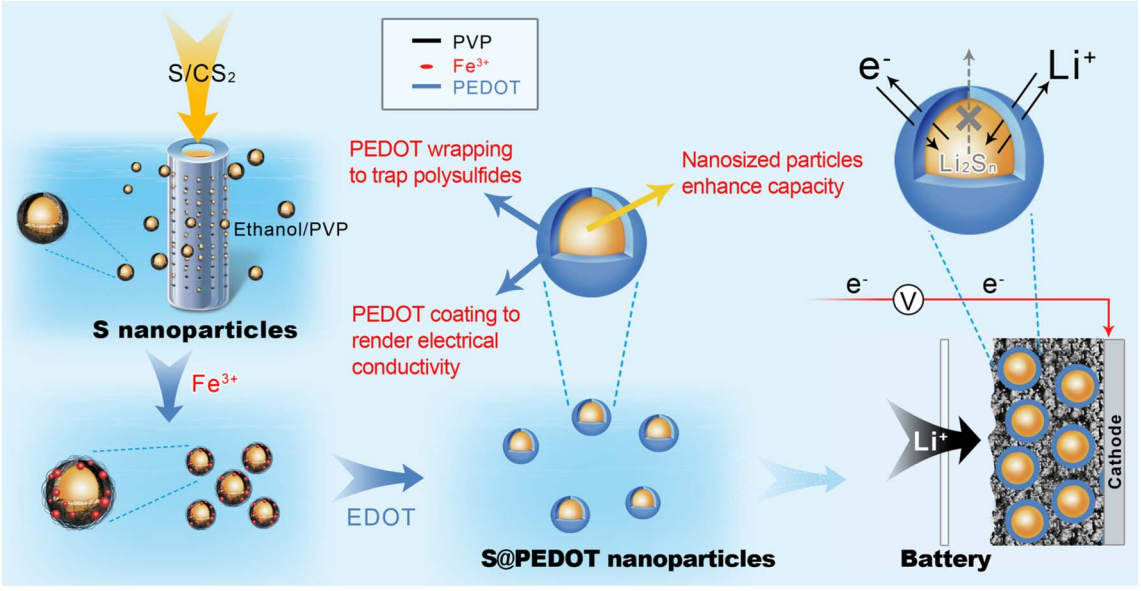

Figure 1 | Schematic iillustration of the preparation of S/PEDOT core/shell nanoparticles and their application as cathode materials for Li/S batteries. Left panel: synthesis of S nanoparticles with the membrane-assisted precipitation method. Middle panel: encapsulation of the S nanoparticles with PEDOT shell via oxidation polymerization. Right panel: S/PEDOT core/shell nanoparticles as Li/S battery cathode active material allow electron transport and Li ion diffusion but limit the polysulfide shuttling.

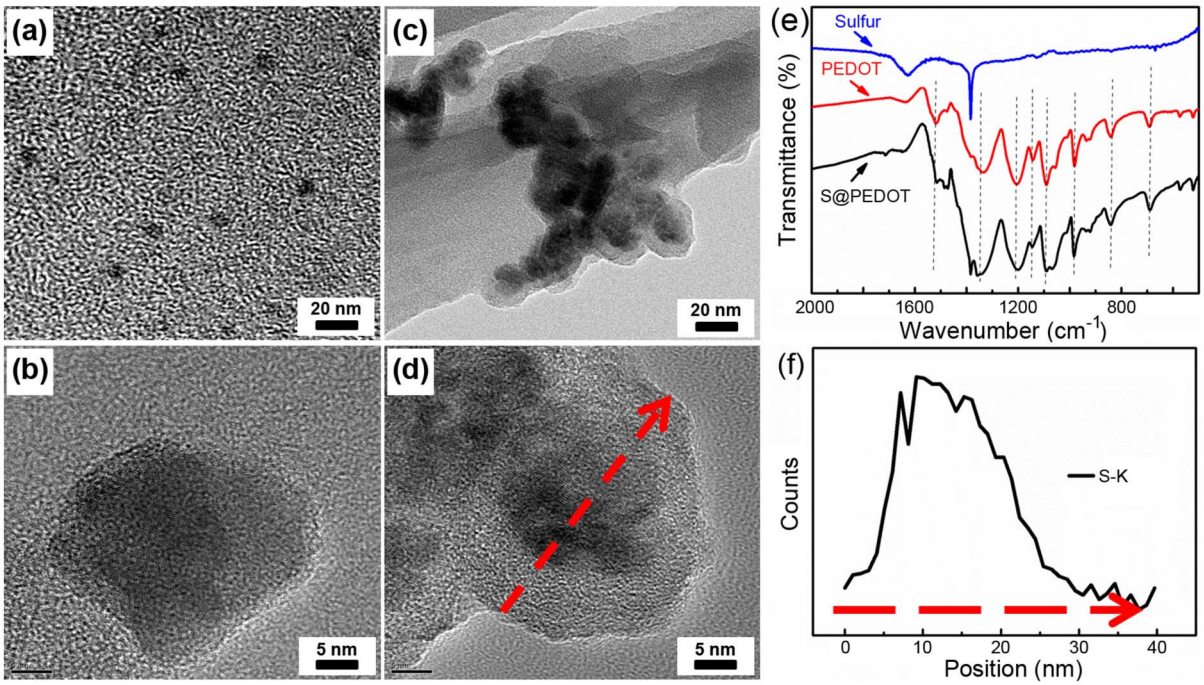

Figure 2 | Structural characterization of S nanoparticles. (a) and (b) TEM images of pure S nanoparticles. (c) and (d) TEM images of S/PEDOT core/shell nanoparticles. (e) FTIR spectrum of the S/PEDOT core/shell nanoparticle. (f) Sulfur elemental content across the S/PEDOT core/shell nanoparticle along the dashed arrow in (d) measured with EDX.

intermediates are very similar for these two samples, however, the nanometer scaled particle size results in a 45% increase in the initial capacity. For Nano-S with smaller particle size and larger specific surface area, more S in the particles can take part in the reduction reaction during the discharge process since the particles are in better contact with the conducting network and more S material is within the electron transfer distance. For CP-S with larger particle size, a part of sulfur is "dead" because it cannot be reached by electrons from the conducting network, which results in low sulfur utilization and less initial discharge capacity than Nano-S[26].

Furthermore, the electrochemical impedance spectra (EIS) of freshly prepared cells at open circuit potential were shown in

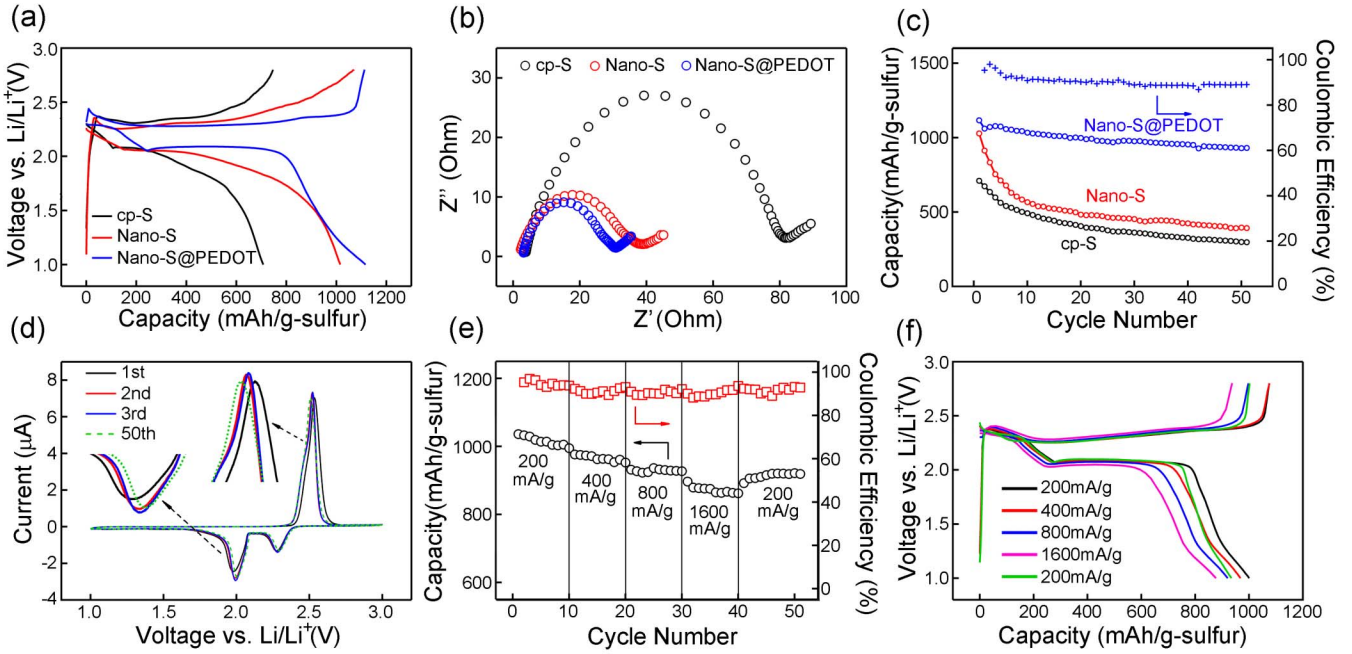

Figure 3 | Electrochemical performance of S nanoparticles. (a) Initial discharge/charge curves of Nano-S@PEDOT (blue), Nano-S (red), and CP-S (black) cathodes at a current density of 400 mA/g (0.25 C). (b) EIS of Nano-S@PEDOT (blue), Nano-S (red), and CP-S (black) cathodes. (c) Discharge capacity and Coulombic efficiency cycling stability for Nano-S@PEDOT (blue), Nano-S (red), and CP-S (black) cathodes at a current density of 400 mA/g. (d) Cyclic voltammogram of Nano-S@PEDOT cathodes at 0.1 mVs^{-1} scanning rate. (e) Rate performance of Nano-S@PEDOT cathodes. (f) Discharge/charge curves of Nano-S@PEDOT cathodes at various current rates.

Figure 3b, the charge-transfer resistance (R_{ct}) of the Nano-S cell (39 Ω) is much smaller than that of the CP-S cell (81 Ω), which corroborates that the nano-size of sulfur particles improves electrochemical kinetic characteristics of sulfur in Li/S batteries. All results above confirm the idea that nanosized sulfur materials facilitate the electrical conduction, improve sulfur utilization and lead to drastic increase in specific capacity.

Effects of conducting polymer encapsulation. Although Nano-S shows much higher initial discharge capacity than CP-S, problems such as high polarization and low cycling stability still exist. These drawbacks can be overcome by encapsulating the Nano-S with conducting PEDOT shells.

First of all, the EIS spectra in Figure 3b show that R_{ct} decreases from 39 Ω (Nano-S) to 31 Ω (Nano-S@PEDOT) after PEDOT encapsulation, which indicates that the conducting PEDOT shell facilitates electrical conduction. Secondly, the PEDOT coating provides an improved reaction environment and helps to push the conversion reactions towards completion in discharge/charge cycles. As shown in Figure 3a and Figure S4, the Nano-S@PEDOT cell show different GDC voltage profile from CP-S and Nano-S cells. Two plateaus at ~2.3 V and ~2.0 V, corresponding to the reduction steps from S_8 to long chain polysulfides (Li_2S_n, $n \geq 4$) and from long chain polysulfides to short chain polysulfides (Li_2S_n, $n < 4$), respectively, are clearly distinguished[27]. The capacity of the upper plateau (2.4 ~ 2.2 V) for Nano-S@PEDOT (244 mAh g^{-1}) is much greater than those for CP-S (105 mAh g^{-1}) and Nano-S (150 mAh g^{-1}), indicating more S_8 molecules obtain electrons and become reduced due to the conductive coating of PEDOT. In addition, Nano-S@PEDOT displays a much more flat and defined lower plateau at ~2.0 V. We speculate that it is because the freshly formed long chain polysulfides are encapsulated in the conducting PEDOT, the abundant electron transfer and Li^+ diffusion paths as well as the relatively uniform reaction environment within the encapsulated particles push the subsequent reduction to short chain polysulfides towards completion before the final reduction step from short chain polysulfides to Li_2S_2 and Li_2S takes place. On the other hand, for CP-S and Nano-S, which are exposed sulfur particles without encapsulation, the reduction steps occur firstly at the sites in contact with the conducting networks. Long chain polysulfides may be reduced to short chain polysulfides and even to insoluble and insulating Li_2S_2 and Li_2S near the contact sites, which may hinder the reduction of polysulfides far away from the contact sites, and thus lead to fast increase of polarization as the discharging proceeds. This is further supported by the EIS curves during the first discharge processes of Nano-S and Nano-S@PEDOT cells (Figure S5). The impedance of the Nano-S cell increases significantly when discharged to below 2.0 V, which may be due to the diffusion/migration of polysulfide to the Li anode forming insulated Li_2S_2 and Li_2S. For Nano-S@PEDOT cell, the PEDOT shell will restrict the polysulfide from diffusion/migration and hence the impedance of Nano-S@PEDOT cell can be well controlled.

Importantly, the PEDOT encapsulation not only promotes the charge/discharge performance of Li/S batteries, but also increases their cycling stability. As shown in Figure 3c, both CP-S and Nano-S cells show quickly fading capacities with the increasing of cycle number at 400 mA/g rate. After 10 cycles, the capacity of CP-S and Nano-S decrease to 69% and 55% of their initial capacities, respectively. However, the reversible capacity of Nano-S@PEDOT cell remains at 930 mAh g^{-1} (with Coulombic efficiency of 90%) after 50 cycles at 400 mA/g, which is 83% of the initial discharge capacity. The cyclic voltammetry (CV) profile of S@PEDOT cell also indicates the excellent reversibility, as shown in Figure 3d, two distinct reduction peaks at about 2.28 V and 1.98 V, and one sharp oxidation peak at about 2.53 V. The two reduction peaks are shifted to slightly higher potential (2.28 V to 2.30 V, 1.98 V to 2.00 V) and the oxidation peak to lower potentials (2.53 V to 2.50 V) after 50 cycles, while the shape and intensity of peaks change little. The R_{ct} of the Nano-S@PEDOT cell increases only slightly even after 50 cycles (Figure S6). An important reason for improved cycle performance is that the PEDOT encapsulation restricts the polysulfides diffusion, which alleviates self-discharging and the shuttle effects, as evidenced by a nearly 100% first charging to discharging capacity ratio and high Coulombic efficiencies in the following cycles. The restriction of polysulfides diffusion is evidenced by the X-ray photoelectron spectroscopy (XPS) results in Fig. S7 showing that the S content on the Li anode surface increases quickly with cycling in the Nano-S cell, while it is stable in the Nano-S@PEDOT cell. Another potential reason for good cycling stability of Nano-S@PEDOT is that the volume change during electrochemical cycling can be well tolerated. Because of the ultrasmall size of S nanoparticles (10 ~ 20 nm in diameter), the 80% volume change of S nanoparticles during electrochemical cycles exerts relatively little stress on the PEDOT shell[28].

Rate performance. Since the conducting PEDOT encapsulation on S nanoparticles provides good electric contact to S nanoparticles and the S nanoparticles have much lower resistance than bulk S, the Nano-S@PEDOT exhibit good rate performances. As shown in Figure 3e, the Nano-S@PEDOT cell shows a reversible capacity of 880 mAh g^{-1} at 1600 mA/g after more than 40 cycles at various rates. Further cycling at 200 mA/g brings it back to a reversible capacity of 920 mAh g^{-1} for another 10 cycles. It needs to be noticed that the Coulombic efficiencies remain stable (~90%) regardless of the discharge/charge rates.

In order to study the electrochemical process of Nano-S@PEDOT at different current rate while excluding the influence of capacity fading, the galvanostatic discharge profiles (Figure 3f) are normalized according to the discharge capacity at each current rate. The normalized profiles in Figure S8 show the two typical discharge plateaus for all curves at different current rates with little increase in voltage polarization as the current rate increase from 200 mA/g to 1600 mA/g (0.125C to 1C). In the normalized rate discharge curves, the capacity corresponding to the upper plateau (~2.3 V) remains nearly the same with the increasing current rate, while the capacity of the lower plateau (~2.0 V) decreases with increasing the current rate. This is because the fast electron transfer lead to the fast formation of insoluble Li_2S_2 and Li_2S, which hinders the complete transition from Li polysulfides to Li_2S_2 and Li_2S[29].

Discussion

Elementary sulfur is a van der Waals solid typically composed of ring-shaped S_8 molecules. Previous reports of S particles were prepared via reduction of $Na_2S_2O_3$ with acid[30]. The formation of S nanoparticle thus involves the reduction of S(II) to S(0), stepwise bonding of S atoms to form S_8 molecules, and then the nucleation and growth of S particles from S_8 molecules. It is difficult to understand and control the thermaldynamics and kinetics of all these elemental steps that may influence the nucleation and growth of S particles. Our report here demonstrates a much simpler approach, which involves only physical precipitation but no chemical reaction. Moreover, since the membrane-assisted precipitation technique is simple and low energy consumption, it may have attractive prospects in large scale production.

The S/PEDOT core/shell nanoparticle shows great electrochemical performance when it is used as the cathode material for Li/S battery. The most important reason is that the particle size is reduced to the nanometer scale. Therefore S nanoparticles have better contact with the conducting network and electrons can transport across the S nanoparticles easier, which enhances the utilization of sulfur. Secondly, conducting PEDOT encapsulation provides better electric contact and limits the dissolution of lithium polysulfide ions and the shuttling effect during cycling. In addition, the PEDOT shell can

prevent aggregation of sulfur particles. Lastly, the PEDOT shells can endure the 80% volume change during the charge/discharge of S nanoparticles, which ensures good contact of S and conducting shells. While there have been some reports of various core/shell cathode materials recently[22,31,32], here we clearly demonstrated for the first time the great potential of nano-size effect in enhancing capacity of Li/S batteries. The high specific capacity and good cycling stability reported here is among the best performances of Li/S cathode materials.

We believe that the performance of the sulfur nanoparticles/conducting polymer cathode materials may be further improved by tuning the size of sulfur nanoparticles and/or the type and amount of the polymer coating. By controlling synthesis parameters such as the concentration of S in CS_2, pore size of the microfiltration membrane and the pumping speed, the size of S nanoparticles can be tailored. Investigations on the tuning of S particle size is currently underway and will be reported in the future.

The amount of PEDOT shell significantly impacts the electrochemical performance of Li/S battery. We have prepared three samples with different amount of PEDOT shell on the S nanoparticle. The compositions of the three samples were measured with the EDX method and the results is listed in Table S1. The cylcing test shows that the Nano-S@PEDOT-2 sample, which contains medium amount of PEDOT (28%) shows the best capacity and cycling stability (Figure S9). We speculate that in the low PEDOT content sample such as the 15% sample Nano-S@PEDOT-1, a portion of the sulfur particles are incompletely encapsulated, thus it displays a good high initial capacity but low cycle stability. On the other hand, high PEDOT content sample such as the 53% sample Nano-S@PEDOT-3 may have too thick PEDOT coating, which may hider electron transport and/or Li^+ diffusion, thus result in overall low performance.

In summary, sulfur nanoparticles with the size about 10 to 20 nm were prepared via a membrane-assisted precipitation technique, and a conducting PEDOT layer was grown on the surface of S nanoparticles to forming S/PEDOT core/shell nano-composites. The high specific surface area of sulfur nanoparticles and the coverage of PEDOT shells provide abundant electron transport active sites which enable the quick transfer of electrons. The conducting PEDOT shells also play an important role as protective layer which effectively prevent soluble lithium polysulfides from dissolving into electrolyte during battery cycling. As a result, the Nano-S@PEDOT cathode material shows excellent sulfur utilization, cyclic durability, and the rate performance. The initial discharge capacity of the Nano-S@PEDOT cathode is 1117 $mAhg^{-1}$ corresponding to a 70% sulfur utilization; and a stable capacity of 930 mAh g^{-1} is retained after 50 cycles.

Methods

Chemicals and materials. Sulfur powder (analytical grade), carbon disulfide (analytical grade), anhydrous ethanol (analytical grade) and ferric chloride (analytical grade) were purchased from Sinopharm Chemical Reagent Co., Ltd. Polyvinyl pyrrolidone and 3,4-Ethylenedioxythiophene were purchased from Sigma-aldrich.

Synthesis of sulfur nanoparticles. Sulfur powder was dissolved carbon disulfide to form S/CS_2 solution (50 mg/ml), and then the solution was pumped into the hollow-fiber membrane module (friendly provided by Zhejiang University) with a metering pump under 5 ml/min speed. The module is submerged in an ethanol solution containing PVP (2.5 g/L). After 5 ml S/CS_2 solution was pumped into the ethanol solution under vigorous stirring (800 r/min), the mixed solution was centrifuged at 15000 rpm for 20 min to separate the sulfur nanoparticles.

Synthesis of Nano-S@PEDOT nano-composites. The as-prepared sulfur nanoparticles were added to 250 ml of deionized water and stirred for about 2 hours (800 r/min). Different amounts of $FeCl_3$ ($FeCl_3$/EDOT 3 : 1 mol/mol) were then added, and the mixture was stirred for another hour. Different amount of EDOT monomer (0.21 ml, 0.45 ml, 0.6 ml correspond to Nano-S@PEDOT-1, Nano-S@PEDOT-2, Nano-S@PEDOT-3) were dissolved in 10 ml of deionized water containing 0.025 g PVP, and then the solution was slowly added to the S nanoparticle solution mixed with $FeCl_3$ to carry out the polymerization. The mixed solution was stirred for 24 h at room temperature. After polymerization, 100 mL of 1 M hydrochloric acid was added, and then the remaining solid was collected and rinsed with deionized water until a neutral pH was reached. The product was dried at 50°C for 48 h under vacuum to give the Nano-S@PEDOT nano-composites.

Cell assembly and testing. Coin-type (CR2025) cells were fabricated by sandwiching a porous polypropylene separator between a cathode containing the active materials and a lithium metal foil in a high-purity argon-filled glove box to avoid contamination by moisture and oxygen. The cathode mixture was prepared by mixing the active material, carbon black, and LA-132 latex binder (Indigo, China) at a weight ratio of 7 : 2 : 1 in deionized water to form slurry. The resultant slurry was uniformly spread on pure aluminum foil with a doctor blade and dried at 50°C for 48 hours under vacuum. The mass loading of sulfur in the best Nano-S@PEDOT (72% S content) electrode is 1.66 mg/cm^2. The electrolyte used was 1 M LiTFSI in a solvent mixture of DOL/DME (1 : 1 v/v). The cells were discharged and charged on a battery test system (NEWARE, NEWARE technology Ltd. Shenzhen) from 1.0 to 2.8 V at a current density of 400 mA/g to test the cycle life.

Characterizations. The sizes of the particles were determined by dynamic light scattering using a Nanophox (Sympatec, Germany). The nanoparticle samples were characterized using a Scanning Electron Microscope (SEM) (FEI Quanta 400 FEG) equipped with Energy Dispersive X-ray Microanalysis (EDX) (Apollo 40 SDD). Fourier transform infrared (FTIR) spectra were collected using a Thermo Scientific Nicolet 6700 spectrometer by dispersing samples in KBr pellets. Transmission electron microscope (TEM) images were recorded using a Tecnai G2 F20 S-TWIN at 200 kV. Cyclic voltammetry (CV) scans were performed on a CHI 660C electrochemical workstation (CHI Instruments, Inc.) with a voltage range from 1.0 to 3.0 V at a scan rate of 0.1 mVs^{-1}. The AC impedance was measured with freshly prepared cells at the open circuit potential (OCP), using an AutoLab (PGSTAT302N) electrochemical workstation. The AC testing voltage amplitude was ±5 mV, and the frequency ranged from 100 kHz to 0.1 Hz.

1. Bruce, P. G., Freunberger, S. A., Hardwick, L. J. & Tarascon, J. M. Li-O_2 and Li-S batteries with high energy storage. *Nat. Mater.* **11**, 19–29 (2012).
2. Yang, Y. *et al.* High-Capacity Micrometer-Sized Li_2S Particles as Cathode Materials for Advanced Rechargeable Lithium-Ion Batteries. *J. Am. Chem. Soc.* **134**, 15387–15394 (2012).
3. Su, Y.-S. & Manthiram, A. Lithium-sulphur batteries with a microporous carbon paper as a bifunctional interlayer. *Nat. Commun.* **3**, 1166 (2012).
4. Schuster, J. *et al.* Spherical Ordered Mesoporous Carbon Nanoparticles with High Porosity for Lithium-Sulfur Batteries. *Angew. Chem. Int. Edit.* **51**, 3591–3595 (2012).
5. Wei, S. Z. *et al.* Sulphur–TiO_2 yolk–shell nanoarchitecture with internal void space for long-cycle lithium–sulphur batteries. *Nat. Commun.* **4**, 1331 (2013).
6. Rauh, R. D., Shuker, F. S., Marston, J. M. & Brummer, S. B. Formation of lithium polysulfides in aprotic media. *J. Inorg. Nucl. Chem.* **39**, 1761–1766 (1977).
7. Mikhaylik, Y. V. & Akridge, J. R. Polysulfide shuttle study in the Li/S battery system. *J. Electrochem. Soc.* **151**, A1969–A1976 (2004).
8. Cheon, S. E. *et al.* Rechargeable lithium sulfur battery - II. Rate capability and cycle characteristics. *J. Electrochem. Soc.* **150**, A800–A805 (2003).
9. Cheon, S. E. *et al.* Structural factors of sulfur cathodes with poly(ethylene oxide) binder for performance of rechargeable lithium sulfur batteries. *J. Electrochem. Soc.* **149**, A1437–A1441 (2002).
10. Li, G. C., Li, G. R., Ye, S. H. & Gao, X. P. A Polyaniline-Coated Sulfur/Carbon Composite with an Enhanced High-Rate Capability as a Cathode Material for Lithium/Sulfur Batteries. *Adv. Energy Mater.* **2**, 1238–124 (2012).
11. Wang, J. L. *et al.* Sulfur composite cathode materials for rechargeable lithium batteries. *Adv. Funct. Mater.* **13**, 487–492 (2003).
12. Han, S. C. *et al.* Effect of multiwalled carbon nanotubes on electrochemical properties of lithium sulfur rechargeable batteries. *J. Electrochem. Soc.* **150**, A889–A893 (2003).
13. Ji, X. L. & Nazar, L. F. Advances in Li-S batteries. *J. Mater. Chem.* **20**, 9821–9826 (2010).
14. Ji, X. L., Lee, K. T. & Nazar, L. F. A highly ordered nanostructured carbon-sulphur cathode for lithium-sulphur batteries. *Nat. Mater.* **8**, 500–506 (2009).
15. Xin, S. *et al.* Smaller Sulfur Molecules Promise Better Lithium-Sulfur Batteries. *J. Am. Chem. Soc.* **134**, 18510–18513 (2012).
16. Wang, H. L. *et al.* Graphene-Wrapped Sulfur Particles as a Rechargeable Lithium-Sulfur Battery Cathode Material with High Capacity and Cycling Stability. *Nano Lett.* **11**, 2644–2647 (2011).
17. Li, N. W. *et al.* High-rate lithium-sulfur batteries promoted by reduced graphene oxide coating. *Chem. Commun.* **48**, 4106–4108 (2012).
18. Evers, S. & Nazar, L. F. Graphene-enveloped sulfur in a one pot reaction: a cathode with good coulombic efficiency and high practical sulfur content. *Chem. Commun.* **48**, 1233–1235 (2012).
19. Xiao, L. F. *et al.* A Soft Approach to Encapsulate Sulfur: Polyaniline Nanotubes for Lithium-Sulfur Batteries with Long Cycle Life. *Adv. Mater.* **24**, 1176–1181 (2012).
20. Raveta, N. *et al.* Electroactivity of natural and synthetic triphylite. *J. Power Sources* **97–98**, 503–507 (2001).
21. Hsu, K.-F., Tsay, S.-Y. & Hwang, B.-J. Synthesis and characterization of nano-sized $LiFePO_4$ cathode materials prepared by a citric acid-based sol-gel route. *J. Mater. Chem.* **14**, 2690–2695 (2004).

22. Fu, Y. Z. & Manthiram, A. Core-shell structured sulfur-polypyrrole composite cathodes for lithium-sulfur batteries. *RSC Adv.* **2**, 5927–5929 (2012).
23. Chen, G. G., Luo, G. S., Xu, J. H. & Wang, J. D. Membrane dispersion precipitation method to prepare nanopartials. *Powder Technol.* **139**, 180–185 (2004).
24. Shin, H. J., Jeon, S. S. & Im, S. S. CNT/PEDOT core/shell nanostructures as a counter electrode for dye-sensitized solar cells. *Synthetic Met.* **161**, 1284–1288 (2011).
25. Zhou, W. C. *et al*. Synthesis and Electromagnetic, Microwave Absorbing Properties of Core-Shell Fe_3O_4-Poly(3, 4-ethylenedioxythiophene) Microspheres. *ACS Appl. Mater. Inter.* **3**, 3839–3845 (2011).
26. Yamin, H. & Peled, E. Electrochemistry of a nonaqueous lithium/sulfur cell. *J. Power Sources* **9**, 281–287 (1983).
27. Jayaprakash, N., Shen, J., Moganty, S. S., Corona, A. & Archer, L. A. Porous Hollow Carbon@Sulfur Composites for High-Power Lithium-Sulfur Batteries. *Angew. Chem. Int. Edit.* **50**, 5904–5908 (2011).
28. Yang, Y., Zheng, G. Y. & Cui, Y. Nanostructured sulfur cathodes. *Chem. Soc. Rev.* **42**, 3018–3032 (2013).
29. Liu, X. F. *et al*. Graphene/Single-Walled Carbon Nanotube Hybrids: One-Step Catalytic Growth and Applications for High-Rate Li–S batteries. *ACS Nano* **6**, 10759–10769 (2012).
30. Chaudhuri, R. G. & Paria, S. Synthesis of sulfur nanoparticles in aqueous surfactant solutions. *J. Colloid Interf. Sci.* **343**, 439–446 (2010).
31. Wu, F. *et al*. Sulfur/Polythiophene with a Core/Shell Structure: Synthesis and Electrochemical Properties of the Cathode for Rechargeable Lithium Batteries. *J. Phys. Chem. C* **115**, 6057–6063 (2011).
32. Qiu, L., Zhang, S., Zhang, L., Sun, M. & Wang, W. Preparation and enhanced electrochemical properties of nano-sulfur/poly(pyrrole-co-aniline) cathode material for lithium/sulfur batteries. *Electrochim. Acta* **55**, 4632–4636 (2010).

Acknowledgments

We acknowledge funding support by National Basic Research Program of China (2010CB934700), National Natural Science Foundation of China (21273273), Knowledge Innovation Program (No.KJCX2-YW-H21) of Chinese Academy of Sciences, Science & Technology Projects of Suzhou (ZXJ2012045). L.C. thanks the Chinese Academy of Sciences Hundred Talents program. We appreciate the electron microscopy facility at SINANO for support on SEM/TEM and EDX measurements.

Author contributions

H.W.C. and L.W.C. designed and conducted the research. W.L.D., J.G. and C.H.W. performed the electrochemical experiments. H.W.C., X.D.W., W.L. and L.W.C. involved in the scientific discussions. H.W.C., W.L. and L.W.C. wrote the paper.

Additional information

Supplementary information accompanies this paper at http://www.nature.com/scientificreports

Competing financial interests: The authors declare no competing financial interests.

How to cite this article: Chen, H. *et al*. Ultrafine Sulfur Nanoparticles in Conducting Polymer Shell as Cathode Materials for High Performance Lithium/Sulfur Batteries. *Sci. Rep.* **3**, 1910; DOI:10.1038/srep01910 (2013).